JOURNAL OF VIROLOGY, Nov. 1992, p. 6655–6667
0022-538X/92/116655-13$02.00/0

Vol. 66, No. 11

Transcriptional Analysis of Multigene Family 110 of African Swine Fever Virus

FERNANDO ALMAZÁN, JAVIER M. RODRÍGUEZ, GERMÁN ANDRÉS, RICARDO PÉREZ, ELADIO VIÑUELA, AND JOSE F. RODRIGUEZ*

Centro de Biología Molecular (Consejo Superior de Investigaciones Científicas-Universidad Autónoma de Madrid), Facultad de Ciencias, Universidad Autónoma de Madrid, Cantoblanco, 28049 Madrid, Spain

Received 22 June 1992/Accepted 18 August 1992

A transcriptional analysis of the 3.2-kb region of the African swine fever virus genome containing the five members of the multigene family 110 is presented. The mRNAs corresponding to the genes studied have short leader sequences with no intervening AUG codons before the translational start site, and their 3′ ends map within a conserved sequence motif formed by a stretch of seven or more consecutive thymidylate residues. The possible role of this sequence as a signal for the 3′-end formation of African swine fever virus mRNAs is discussed. While four of the genes studied are actively transcribed from the beginning of the infection until the onset of virus DNA replication, the transcription of one of the members of the multigene family 110, the L270 gene, is silenced at an earlier time. A detailed analysis, including in vitro translation of mRNAs isolated from infected Vero cells, revealed that the L270 gene belongs to a small subset of early genes, designated immediate early, whose transcription is silenced before the onset of virus DNA replication. The transcriptional data obtained enabled us to generate the first detailed transcriptional map of a region of the African swine fever virus genome, thus opening the possibility of studying the *cis*-acting sequences involved in transcriptional control of the viral genes.

African swine fever virus (ASFV), formerly considered a member of the *Iridoviridae* family, is the only representative of an unnamed family of animal DNA viruses. ASFV infects soft ticks of the *Ornithodoros* genus, as well as members of the Suidae family, including domestic pigs (28). Efforts to control the spread of ASFV are largely complicated by the lack of effective vaccines (27). Thus, for many countries worldwide, African swine fever is still a major animal health concern.

ASFV particles are formed by large icosahedral capsids, similar to those of iridovirus (1, 14), wrapped by a lipoprotein membrane. The virus genome, a single molecule of double-stranded DNA of approximately 170 kb with covalently linked ends, associates with a number of proteins, forming an electron-dense structure, the virus core, located inside the capsid (reviewed in reference 25). Transcription of ASFV genes is carried out by the virus-encoded enzymatic machinery (10), giving rise to mature transcripts that have a structure similar to that of other eukaryotic mRNAs, containing capped 5′ ends and poly(A) tails at their 3′ termini (20). On the basis of their temporal regulation, ASFV genes have been grouped into two major categories: early genes, transcribed immediately after the beginning of the infectious cycle, and late genes, whose transcription is dependent upon replication of the virus DNA (21). Although the nucleotide sequences of a relatively large number of genes have been reported, little is known about their transcription. The first described ASFV transcriptional maps were generated by cell-free translation of virus mRNAs selected by hybridization to different genomic fragments (21). More recently, Northern (RNA) blot hybridization techniques have been applied to study the transcription of several ASFV genes (2, 7, 18). These studies have provided a broad view of the transcriptional activity of different regions of the virus genome. However, the lack of detailed transcriptional maps has hampered progress towards understanding of the mechanisms that govern the expression of the virus genes.

We have carried out a thorough transcriptional analysis of a 3.2-kb region located within the left end of the genome of Vero cell-adapted ASFV strain BA71V. This DNA region contains five open reading frames (ORFs) that correspond to the members of the multigene family 110 of ASFV (2). Transcription of these tandemly arranged genes takes place immediately after the onset of infection (2). Thus, this DNA region appeared to be a good candidate for the study of ASFV early transcription. The results reported here provide new information regarding the transcription of ASFV early genes.

MATERIALS AND METHODS

Cells and virus. Vero cells, obtained from the American Type Culture Collection, were routinely grown in Dulbecco's modified Eagle's medium containing 10% fetal bovine serum. ASFV strain BA71V was propagated and titrated as previously described (6). Virus inoculation of cell cultures grown in 100-mm-diameter plastic petri dishes was carried out at 4°C for 2 h by using 25 PFU per cell. For this, virus stocks were diluted in Dulbecco's modified Eagle's medium lacking sodium bicarbonate and supplemented with 25 mM *N*-2-hydroxyethylpiperazine-*N*′-2-ethanesulfonic acid (HEPES), pH 7.0. After inoculation, the monolayers were washed twice with normal Dulbecco's modified Eagle's medium containing 2% fetal bovine serum and then incubated at 37°C under 7% CO_2 until processing.

Preparation of RNA. RNA was obtained as previously described (22). Briefly, after removal of the medium, cells were scraped and suspended in chilled phosphate-buffered saline. After centrifugation at low speed for 5 min, the cell

* Corresponding author.

pellets were suspended in lysis buffer (4 M guanidinium thiocyanate, 0.1 M Tris HCl [pH 7.5], 1% β-mercaptoethanol), layered on top of a 3-ml cushion of 5.7 M cesium chloride containing 10 mM EDTA, and spun at 300,000 × *g* for 18 h. The RNA pellets were suspended in H_2O pretreated with diethyl pyrocarbonate (0.2%) containing 1% sodium dodecyl sulfate and ethanol precipitated twice. The RNAs were finally suspended in diethyl pyrocarbonate-pretreated H_2O at a concentration of 2 mg/ml and stored at −70°C.

Preparation of ^{32}P-end-labeled probes. All of the ^{32}P-end-label DNA probes used were prepared by using plasmid p*Hin*dIIIC/*Sal*IG (2). The plasmid was purified twice by centrifugation in CsCl gradients by following a standard protocol (22). For labeling of the 5′ ends, the DNA fragments were dephosphorylated with calf intestinal phosphatase and then treated with polynucleotide kinase in the presence of [γ-^{32}P]ATP. Labeling of the 3′ DNA ends was performed with Klenow enzyme by using the α-^{32}P-labeled deoxynucleoside triphosphate corresponding to the first nucleotide required for the end-filling reaction. After labeling, the ^{32}P-end-labeled DNA fragments were purified from agarose gels by electroelution with a unidirectional electroelution apparatus (International Biotechnologies, Inc., New Haven, Conn.). The restriction enzymes used for generation of the probes are described in the corresponding figures (see Fig. 2 to 6).

S1 nuclease analysis. S1 nuclease analysis was done as previously described (22), with minor modifications. Approximately 5 × 10^3 cpm of the relevant ^{32}P-end-labeled probe was mixed with 7.5 μg of total RNA and then ethanol precipitated. The DNA-RNA pellets were thoroughly suspended in 30 μl of hybridization buffer [40 mM piperazine-*N*,*N*′-bis(2-ethanesulfonic acid) (PIPES; pH 6.4), 1 mM EDTA, 0.4 M NaCl, 80% formamide]. The samples were heated at 75°C for 5 min and then incubated at 37°C for 18 h. After hybridization, 300 μl of digestion buffer (28 mM NaCl, 5 mM sodium acetate [pH 4.3], 0.45 mM $ZnSO_4$, 20 μg of single-stranded DNA per ml) containing 10^3 U of S1 nuclease (Boehringer Mannheim GmbH) per ml was added and the samples were incubated for 1 h at 25°C. S1 nuclease digestion was stopped by adding 70 μl of ice-cold stop buffer (4 M ammonium acetate, 100 mM EDTA). Samples were phenol extracted and ethanol precipitated, and the pellets were suspended in 15 μl of H_2O. After addition of 5 μl of loading buffer (50 mM Tris-borate [pH 8.3], 1 mM EDTA, 0.1% xylene cyanol, 0.1% bromophenol blue, 80% formamide), the samples were heated at 90°C for 5 min and loaded in 6% polyacrylamide sequencing gels.

Synthesis, cloning, and sequencing of cDNA. cDNA was synthesized from poly(A)$^+$ selected RNA obtained from ASFV-infected Vero cells maintained in the presence of the inhibitor of DNA replication cytosine arabinoside (AraC; 40 μg/ml). The synthesis was done with a commercial kit (cDNA Synthesis System Plus; Amersham International plc, Amersham, United Kingdom). The cDNA was cloned into *Sma*I-linearized M13mp10 (29), and the resulting cDNA library was screened with a ^{32}P-end-labeled oligonucleotide (5′ CTAAATCATACATACAATTTATCCAGCCAAC 3′) specific for the V118 gene (2). Purification of poly(A)$^+$ RNA, cDNA cloning, preparation of single- and double-stranded DNA templates from the selected M13 clones, and nucleotide sequencing were done as previously described (22).

Cell-free translation of RNA. A 10-μg sample of total RNA, isolated from either mock-infected or ASFV-infected Vero cells, was added to 20 μl of rabbit reticulocyte lysate (Amersham); this mixture was supplemented with 4 μl of 15-mCi/ml (1,163-Ci/mmol) [^{35}S]methionine (Amersham) and then incubated at 30°C for 2 h. After incubation, the samples were treated with 0.1 mg of RNase A per ml in the presence of 10 mM EDTA for 15 min at 37°C and then stored at −70°C until electrophoresis.

2D gel electrophoresis. Two-dimensional (2D) gel electrophoresis was performed as previously described (4, 15), with minor modifications. Isoelectric focusing gels (17 by 0.3 cm) were prepared by using ampholines in the pH ranges 5 to 7 and 3.5 to 10 in a ratio of 5:1 in 3.9% acrylamide. Before loading, the gels were prerun at 700 V for 1.5 h. Protein samples (25 μl) containing 1 × 10^5 to 5 × 10^5 cpm of acid-insoluble [^{35}S]methionine were electrophoresed at 800 V for 18 h and then at 1,000 V for 30 min. Focused gels were incubated for 10 min in equilibration buffer and loaded onto sodium dodecyl sulfate-polyacrylamide gradient (7 to 20%) slab gels. After electrophoresis, the gels were processed for fluorography as previously described (11).

RESULTS

Temporal regulation of early gene transcription. Expression of ASFV genes is temporally regulated (21, 23). However, the precise transcriptional kinetics of virus genes was unknown. Thus, we decided to carry out a careful analysis of early gene transcription in ASFV-infected Vero cells. For this, the V118 gene, a member of the multigene family 110 (see Fig. 7A), was selected. The presence of V118 transcripts within infected cells at different times postinfection was estimated by assaying the proportion of a V118-specific ^{32}P-5′-end-labeled probe (see Fig. 2A) protected from digestion with S1 nuclease following hybridization to total RNA extracted from virus-infected cells. As shown in Fig. 1, V118-specific transcripts were detectable as early as 2 h postinfection. The levels of transcript then increased rapidly, reaching a plateau that spanned from 4 to 8 h, and then underwent a sudden fall that was coincidental with the onset virus DNA replication (data not shown). It is interesting that a residual amount of V118 transcript was still detectable several hours after the onset of DNA replication, a phenomenon that has also been observed with the transcripts corresponding to three other members of the multigene family 110 (see results below) and with those corresponding to the p32 gene, an ASFV early gene unrelated to the multigene family 110 (16a).

Transcriptional mapping of multigene family 110. The five members of the 110 multigene family are transcribed during the early phase of infection (2). Transcripts corresponding to these five genes have also been detected after incubation of permeabilized virions in the presence of ribonucleotides, indicating that their transcription is carried out in vitro by the virion-associated RNA polymerase (2).

One of the main goals of the work reported here was to generate a detailed transcriptional map of the multigene family 110 by using S1 nuclease analysis (3). For this, a series of ^{32}P-end-labeled probes were generated and hybridized to total RNA isolated at 8 h postinfection from mock-infected Vero cells (uninfected RNA) or virus-infected cultures maintained in the presence of either cycloheximide (immediate-early RNA) or AraC (early RNA) and to RNA isolated at 18 h postinfection (late RNA). Specific probe protection was detected only after hybridization to RNA extracted from infected cell cultures (see Fig. 2 to 6 and 8), and with the exception of the samples corresponding to the L270 gene (see Fig. 8), the highest and lowest levels of

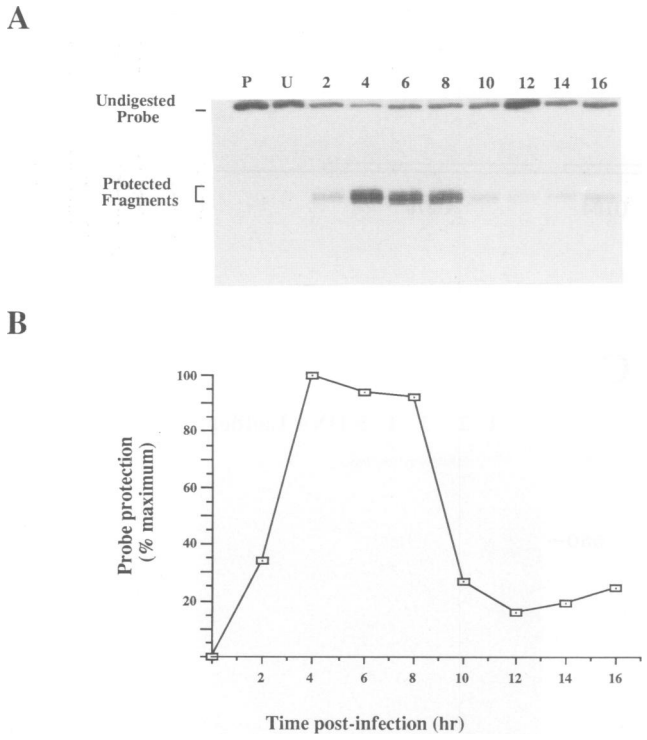

FIG. 1. Transcriptional kinetics of the V118 gene. (A) Detection of V118-specific transcripts by S1 nuclease protection analysis. A ^{32}P-5′-end-labeled probe (see Fig. 2) was allowed to hybridize to 7.5 μg of total RNA extracted from either uninfected (lane U) or ASFV-infected (lanes 2 to 16) Vero cells. The RNA-DNA hybrids were digested with S1 nuclease and subjected to electrophoresis. The positions of both the undigested probe and the specifically protected fragments are indicated. The numbers indicate the times postinfection (hours) at which the different RNA samples were extracted. The sample in lane P corresponds to the undigested probe. (B) Quantitation of the S1 protection analysis. The results shown in panel A were quantitated by densitometry and plotted as a percentage of the maximum level of specific probe protection.

protection were found after hybridization to immediate-early and late RNAs (see Fig. 2 to 6), respectively.

V118. 5′-end mapping of the V118 gene was done with a ^{32}P-end-labeled probe of 171 bases (Fig. 2A). After treatment with S1 nuclease, three specific bands corresponding to protected DNA fragments of 141, 143, and 144 bases were detected (Fig. 2B, lanes 3 to 5). The band corresponding to the smallest DNA fragment (141 bases) constitutes only a minor fraction of the total protection. According to these results, V118 has a transcriptional initiation site located 55 to 56 bases upstream of the initiation codon of the ORF (see Fig. 7). For 3′-end mapping, a ^{32}P-labeled probe of 902 bases was used (Fig. 2A). A ladder of bands corresponding to DNA fragments of 102 to 111 bases and a band of approximately 550 bases was detected (Fig. 2C, lanes 3 and 4). This result shows that two different 3′ ends exist for transcripts from the V118 ORF, located at 50 to 59 and approximately 500 bases downstream of the first nucleotide of the termination codon of the ORF. The position of the most distal 3′ end is consistent with the existence of readthrough transcripts spanning the coding sequences of both the V118 and X′82 genes.

X′82. 5′ mapping of the X′82 ORF was done with a ^{32}P-end-labeled probe of 516 bases (Fig. 3A). Two intense bands corresponding to protected DNA fragments of 91 and 93 bases were detected (Fig. 3B, lanes 3 to 5). A third band corresponding to a DNA fragment of 92 bases was also detected after longer exposure of the autoradiogram. This result indicates the presence of a transcriptional initiation site located 68 to 70 bases upstream of the translational initiation site of X′82 (see Fig. 7). 3′-end mapping of X′82 was performed with a ^{32}P-end-labeled probe of 385 bases (Fig. 3A). As can be observed in Fig. 3C, a small cluster of bands corresponding to protected DNA fragments of 233 to 238 bases was detected (Fig. 3C, lanes 3 and 4), showing that the 3′ ends of transcripts running through the analyzed region map 7 to 12 bases downstream of the first nucleotide of the termination codon of the X′82 ORF (see Fig. 7). The position of these 3′ ends is consistent with the results determining the presence of V118 readthrough transcripts described above (Fig. 2C, lanes 3 and 4).

U124. The S1 nuclease analysis used to determine the 5′ end of the transcripts from the U124 gene was performed with a ^{32}P-end-labeled probe of 532 bases (Fig. 4A) and resulted in detection of three specifically protected bands (Fig. 4B, lanes 3 to 5) corresponding to DNA fragments of 118 to 120 bases. The shortest fragment (118 bases) is clearly more abundant than the longer ones, indicating the existence of an initiation site located 67 to 69 bases upstream of the initiator AUG of the U124 ORF (see Fig. 7). 3′-end mapping of the U124 transcripts was done with a ^{32}P-end-labeled probe of 656 bases (Fig. 4A). After hybridization and S1 digestion, two clusters of protected DNA fragments of approximately 380 to 385 and 405 to 410 bases were detected (Fig. 4C). This result indicates the existence of two different 3′ ends for the transcripts running through the U124 region, which map 29 to 34 and 54 to 59 bases downstream of the first nucleotide of the termination codon of the ORF (see Fig. 7).

U104. The 5′ end of the U104 transcripts was determined by using a ^{32}P-end-labeled probe of 365 bases (Fig. 5A). After digestion with S1 nuclease, six protected bands corresponding to DNA fragments with sizes ranging from 100 to 105 bases were detected (Fig. 5B, lanes 3 to 5). The bands corresponding to fragments of 102 and 103 bases showed a relatively higher intensity, indicating the presence of a major transcriptional initiation site located 11 to 12 bases upstream of the first AUG of this ORF (see Fig. 7). The 3′ end of the U104 transcripts was determined by using a ^{32}P-end-labeled probe of 461 bases (Fig. 5A). After S1 nuclease digestion, a cluster of protected DNA fragments with sizes ranging from 134 to 141 bases was detected (Fig. 5C, lanes 3 to 5). Thus, the 3′ ends of the transcripts corresponding to the U104 gene map 27 to 34 bases downstream of the first nucleotide of the termination codon of the ORF (see Fig. 7).

L270. The 5′ end of L270 was mapped by using a ^{32}P-end-labeled probe of 772 bases (Fig. 6A). S1 nuclease analysis revealed the presence of two protected bands of 124 and approximately 500 bases after hybridization of the probe to immediate-early RNA (Fig. 6B, lane 3) and a single band of 500 bases after hybridization to early RNA (Fig. 6B, lane 4). These results indicate that transcripts running through the region covered by the radioactive probe belong to two different species. The species detected in samples from both early and immediate-early RNAs (approximately 500 bases) corresponds to readthrough transcripts that initiate upstream of the U104 ORF (Fig. 7), while the shorter one (124 bases), detected only in samples from immediate-early RNA, corresponds to authentic L270 transcripts that initiate 68 bases

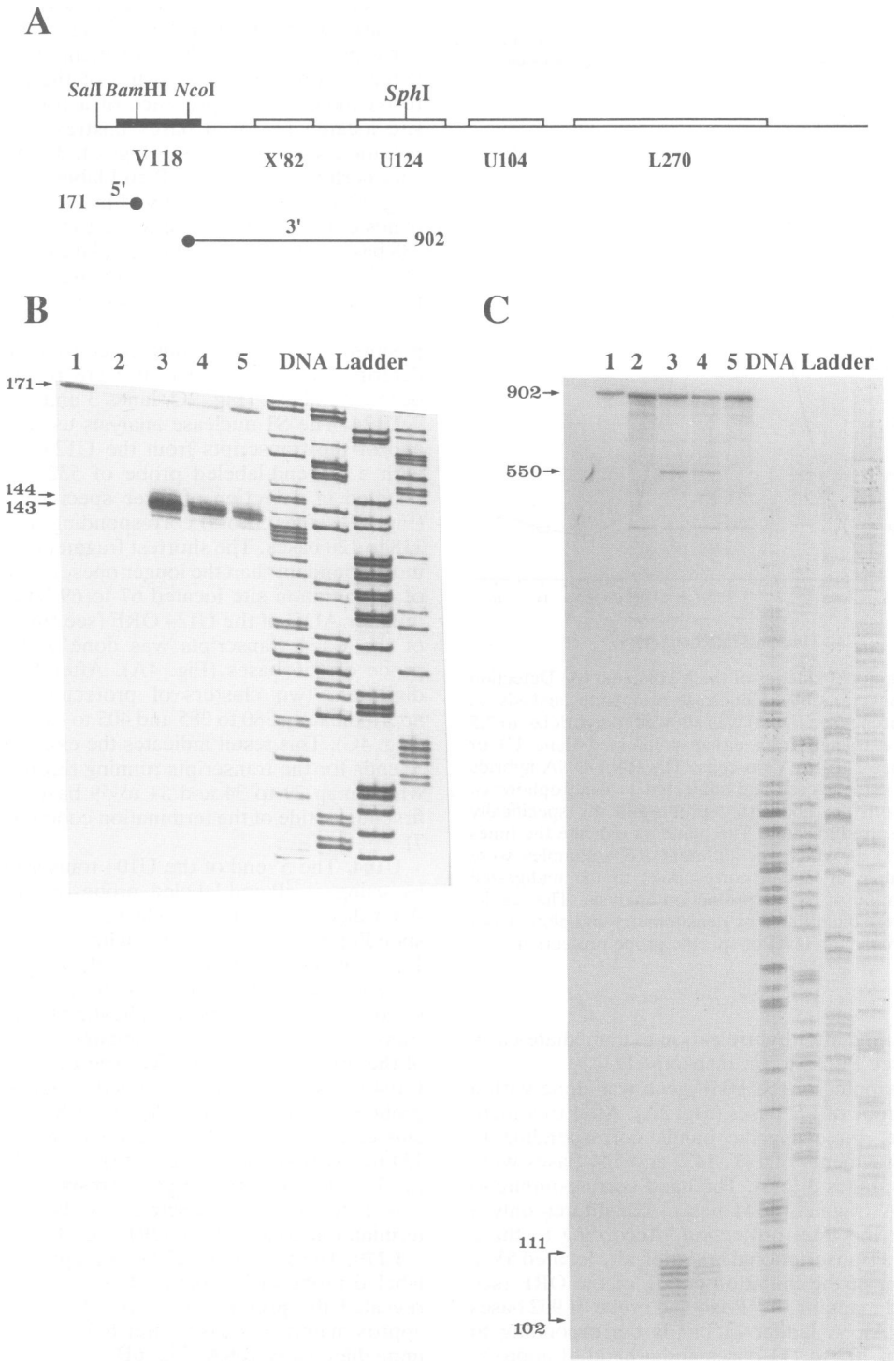

FIG. 2. S1 nuclease mapping of the V118 gene. (A) Diagram showing the relative position of the V118 ORF (solid box) within the *Hin*dIII-*Sal*I G fragment of the *Hin*dIII C fragment of the ASFV genome (2) and the endonuclease restriction enzymes used for generation of the ^{32}P-end-labeled probes used to map both the 5′ and 3′ ends of the gene. The sizes (nucleotides) and relative positions of the labeled probes are indicated. (B) Autoradiogram showing the results of 5′-end mapping of the V118 gene. Lane 1 corresponds to the undigested ^{32}P-end-labeled probe. Lanes 2 to 5 correspond to the samples obtained after S1 digestion of RNA-DNA hybrids generated by incubation of the probe with RNA from uninfected cells and ASFV immediate-early, early, and late RNAs, respectively. After S1 digestion, the samples were electrophoresed alongside an irrelevant DNA sequencing reaction (DNA ladder) used as size markers. The sizes (nucleotides) of both the undigested probe and the S1-protected fragments are indicated. (C) Autoradiogram showing the results of 3′-end mapping of the V118 gene. The notation used is the same as that of panel B.

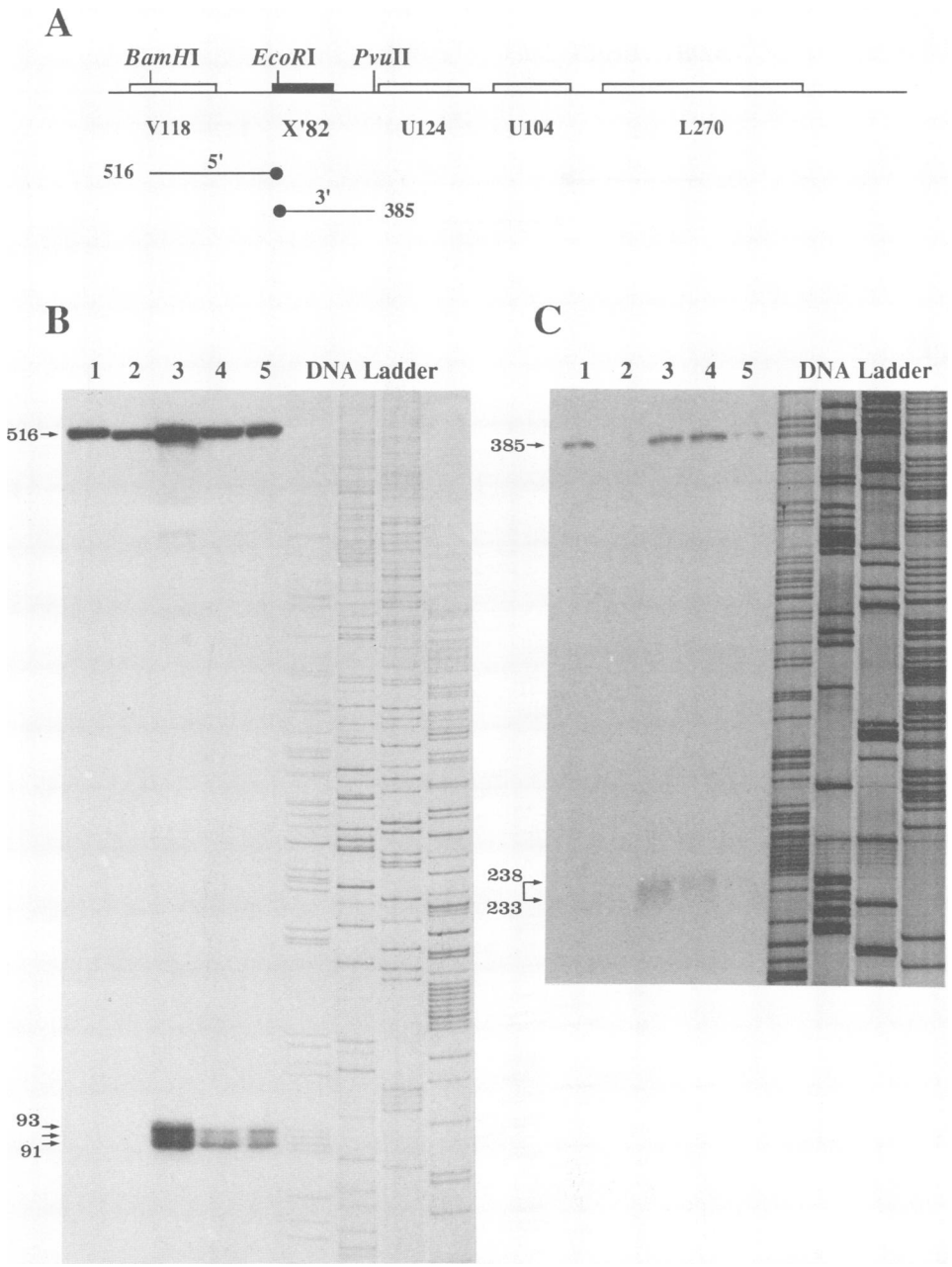

FIG. 3. S1 nuclease mapping of the X'82 gene. (A) Diagram showing the relative position of the X'82 ORF (solid box) within the *Hin*dIII-*Sal*I G fragment of the *Hin*dIII C fragment of the ASFV genome (2) and the endonuclease restriction enzymes used for generation of the ^{32}P-end-labeled probes used to map both the 5' and 3' ends of the gene. The sizes (nucleotides) and the relative positions of the labeled probes are indicated. (B) Autoradiogram showing the results of 5'-end mapping of the X'82 gene. Lane 1 corresponds to the undigested ^{32}P-end-labeled probe. Lanes 2 to 5 correspond to the samples obtained after S1 digestion of RNA-DNA hybrids generated by incubation of the probe with RNA from uninfected cells and ASFV immediate-early, early, and late RNAs, respectively. After S1 digestion, the samples were electrophoresed alongside an irrelevant DNA sequencing reaction (DNA ladder) used as size markers. The sizes (nucleotides) of both the undigested probe and the S1-protected fragments are indicated. (C) Autoradiogram showing the results of 3'-end mapping of the X'82 gene. The notation used is the same as that of panel B.

upstream of the first AUG codon of the L270 ORF (Fig. 7). 3'-end mapping of L270 transcripts was done with a ^{32}P-end-labeled probe of 512 bases (Fig. 6A). After S1 nuclease digestion, three clusters of protected bands corresponding to DNA fragments of 179 to 190, 300 to 310, and 385 to 395 bases were detected in the samples corresponding to early and immediate-early RNAs (Fig. 6C, lanes 3 and 4). This revealed the existence of three different 3' ends located at 3 to 14, 125 to 135, and 209 to 219 bases downstream of the termination codon of the L270 ORF.

Nucleotide sequence of the 3' end of cDNAs from the V118 gene. S1 mapping of the transcripts from the genes under study revealed that in all cases the 3' end of the mRNAs map within a short DNA stretch consisting of seven or more

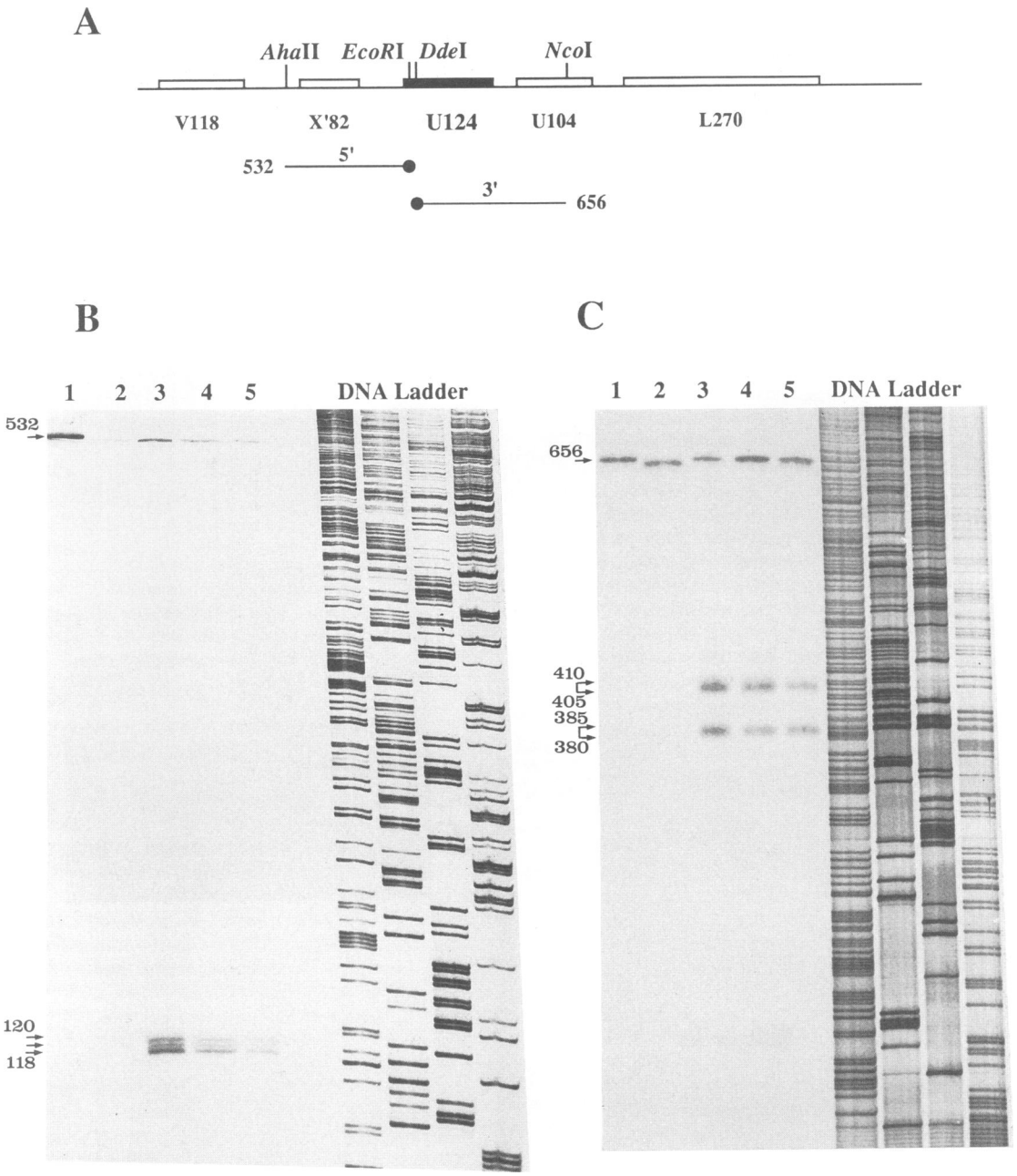

FIG. 4. S1 nuclease mapping of the U124 gene. (A) Diagram showing the relative position of the U124 ORF (solid box) within the *Hin*dIII-*Sal*I G fragment of the *Hin*dIII C fragment of the ASFV genome (2) and the endonuclease restriction enzymes used for generation of the ^{32}P-end-labeled probes used to map both the 5′ and 3′ ends of the gene. The sizes (nucleotides) and relative positions of the labeled probes are indicated. (B) Autoradiogram showing the results of 5′-end mapping of the U124 gene. Lane 1 corresponds to the undigested ^{32}P-end-labeled probe. Lanes 2 to 5 correspond to the samples obtained after S1 digestion of RNA-DNA hybrids generated by incubation of the probe with RNA from uninfected cells and ASFV immediate-early, early, and late RNAs, respectively. After S1 digestion, the samples were electrophoresed alongside an irrelevant DNA sequencing reaction (DNA ladder) used as size markers. The sizes (nucleotides) of both the undigested probe and the S1-protected fragments are indicated. (C) Autoradiogram showing the results of 3′-end mapping of the U124 gene. The notation used is the same as that of panel B.

consecutive thymidylate residues. To rule out the possibility that these results were artifacts caused during digestion with S1 nuclease, a different experimental approach was used. A cDNA library from poly(A)$^+$ ASFV early RNA was generated by using the vector M13mp10. Three M13 clones containing inserts corresponding to the V118 gene were selected by hybridization to a ^{32}P-labeled V118-specific oligonucleotide (see Material and Methods), and the regions corresponding to the 3′ end of the original mRNAs were sequenced (Fig. 8A). As shown in Fig. 8B, the 3′ end of two cDNAs (clones II and III) map to residue 4 of the 7T motif, while that of the third (clone I) maps to residue 6 of the

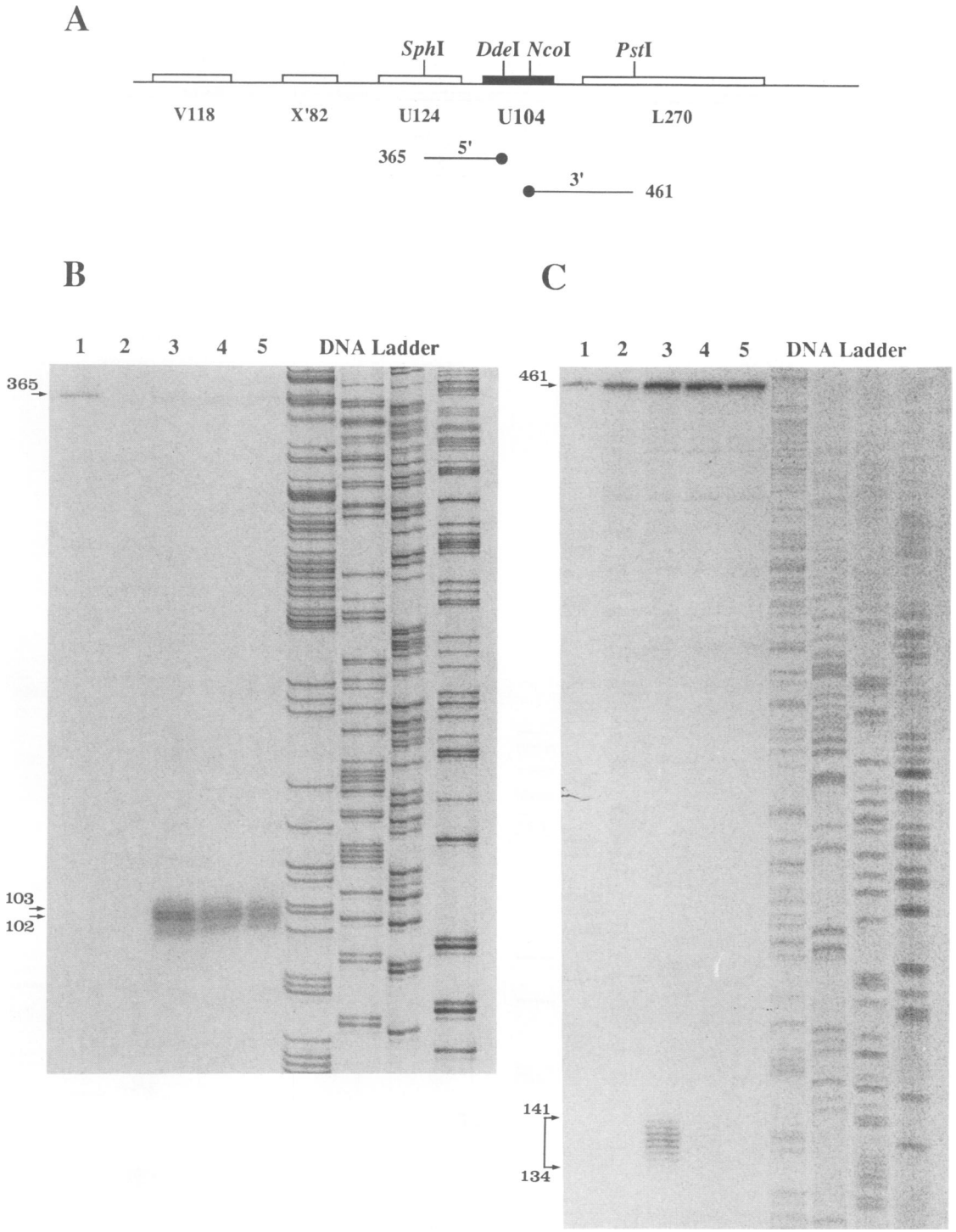

FIG. 5. S1 nuclease mapping of the U104 gene. (A) Diagram showing the relative position of the U104 ORF (solid box) within the *Hin*dIII-*Sal*I G fragment of the *Hin*dIII C fragment of the ASFV genome (2) and the endonuclease restriction enzymes used for generation of the ^{32}P-end-labeled probes used to map both the 5′ and 3′ ends of the gene. The sizes (nucleotides) and relative positions of the labeled probes are indicated. (B) Autoradiogram showing the results of 5′-end mapping of the U104 gene. Lane 1 corresponds to the undigested ^{32}P-end-labeled probe. Lanes 2 to 5 correspond to the samples obtained after S1 digestion of RNA-DNA hybrids generated by incubation of the probe with RNA from uninfected cells and ASFV immediate-early, early, and late RNAs, respectively. After S1 digestion, the samples were electrophoresed alongside an irrelevant DNA sequencing reaction (DNA ladder) used as size markers. The sizes (nucleotides) of both the undigested probe and the S1-protected fragments are indicated. (C) Autoradiogram showing the results of 3′-end mapping of the U104 gene. The notation used is the same as that of panel B.

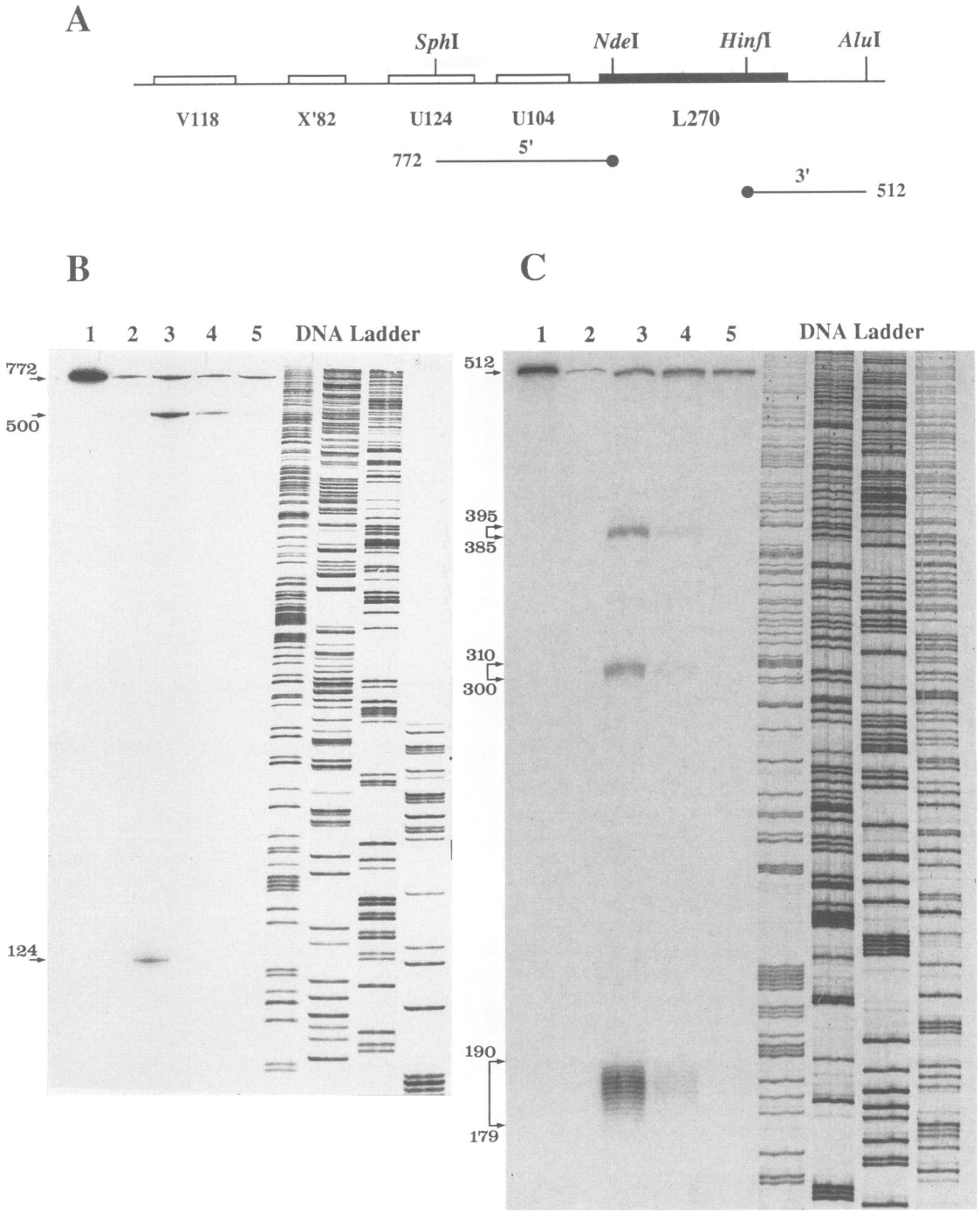

FIG. 6. S1 nuclease mapping of the L270 gene. (A) Diagram showing the relative position of the L270 ORF (solid box) within the *Hin*dIII-*Sal*I G fragment of the *Hin*dIII C fragment of the ASFV genome (2) and the endonuclease restriction enzymes used for generation of the ^{32}P-end-labeled probes used to map both the 5′ and 3′ ends of the gene. The sizes (nucleotides) and relative positions of the labeled probes are indicated. (B) Autoradiogram showing the results of 5′-end mapping of the L270 gene. Lane 1 corresponds to the undigested ^{32}P-end-labeled probe. Lanes 2 to 5 correspond to the samples obtained after S1 digestion of RNA-DNA hybrids generated by incubation of the probe with RNA from uninfected cells and ASFV immediate-early, early, and late RNAs, respectively. After S1 digestion, the samples were electrophoresed alongside an irrelevant DNA sequencing reaction (DNA ladder) used as size markers. The sizes (nucleotides) of both the undigested probe and the S1-protected fragments are indicated. (C) Autoradiogram showing the results of 3′-end mapping of the L270 gene. The notation used is the same as that of panel B.

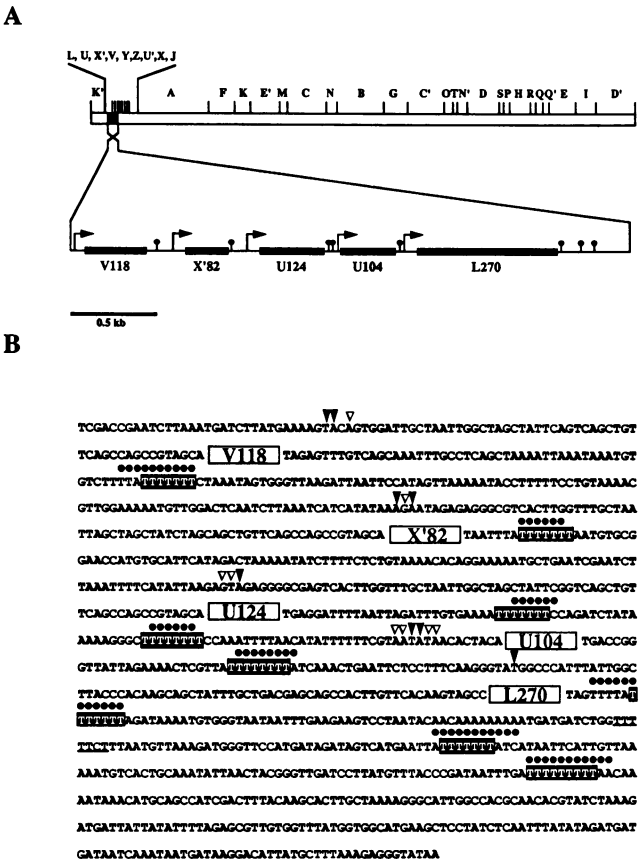

FIG. 7. Transcriptional map of the multigene family 110. (A) The diagram shows the location within the ASFV genome of the 3.2-kb *Hin*dIII-*Sal*I G fragment containing the 110 multigene family and the relative positions of the ORFs corresponding to the members of the multigene family within this fragment (2). The positions of the transcriptional initiation and termination sites detected are indicated by arrows and circles, respectively. The capital letters in the upper part of the diagram represent the locations of the *Eco*RI restriction sites within the genome of the BA71V strain of ASFV. To facilitate comprehension of the diagram, the orientation of the expanded 3.2-kb DNA region has been inverted. (B) The diagram shows the precise location of the transcriptional initiation and termination sites within the nucleotide sequence of the noncoding strand of the DNA region analyzed. The ORFs are indicated by boxes, the solid and empty triangles represent major and minor transcriptional initiation sites, and the circles indicate the locations of transcriptional termination sites.

motif. These results confirm the data obtained by S1 nuclease analysis.

Transcription of L270 is abrogated before the onset of DNA replication. The analysis carried out to determine the 5′ end of L270 transcripts showed that L270 transcripts, initiating immediately upstream of the first AUG of the ORF, were detectable only in immediate-early RNA (Fig. 6B). To further characterize this finding, a more detailed transcriptional analysis of the L270 gene was undertaken. Three different series of S1 nuclease digestions were carried out by using total RNA extracted at short intervals after the beginning of infection from either untreated, AraC-treated, or cycloheximide-treated ASFV-infected cells. Identical amounts of the different RNAs were hybridized to a ^{32}P-end-labeled probe identical to that used for initial characterization of the 5′ end of the L270 ORF (Fig. 6A). The results of this analysis (Fig. 9) demonstrate that while in all three types of RNA the level of U104 readthrough transcripts increased in a time-dependent manner (Fig. 9), the kinetics of accumulation of L270-specific transcripts was affected by cycloheximide treatment. While in both untreated and AraC-treated cultures the levels of L270-specific transcripts reached a maximum at 3 h postinfection and then slowly decreased (Fig. 9), in cells treated with cycloheximide L270 mRNA accumulated with time, reaching a maximum level at the latest time analyzed (6 h postinfection). These results demonstrate that transcription of the L270 gene is silenced much earlier than that of the U104 gene and that this transcriptional silencing does not require virus DNA replication but is dependent on protein synthesis.

L270 belongs to a small subset of the early gene class. The results described above demonstrate that transcription of the L270 gene begins immediately after infection and ceases before the onset of DNA replication. Consequently, the transcriptional kinetics of L270 is different from those observed for the other four genes of the multigene family 110. Therefore, it was of interest to determine whether the transcriptional kinetics of L270 was shared by other virus genes. RNA samples obtained at 8 h postinfection from either mock-infected or ASFV-infected Vero cells treated with either AraC (early RNA) or cycloheximide (immediate-early RNA) were used to direct protein synthesis in rabbit reticulocyte lysates. The polypeptides obtained after in vitro translation of the different RNAs were analyzed by 2D gel electrophoresis. Although the polypeptide patterns obtained after translation of early (Fig. 10D) and immediate-early (Fig. 10C) RNAs were very similar, at least three polypeptides were detectable only after translation of immediate-early RNA (Fig. 10C). The absence of these three polypeptides among the products of translation of early RNA indicates that their corresponding genes follow a transcriptional kinetics similar to that of the L270 gene.

DISCUSSION

The results of time course transcriptional analysis of the V118 gene demonstrate that transcription of this gene undergoes a sharp decline between 8 and 10 h postinfection. These results confirm previous data that indicate that expression of ASFV genes is subjected to strong temporal regulation (21, 23). Interestingly, although a marked decrease in the level of transcripts corresponding to the V118 gene occurs after the onset of virus DNA replication, a low level of V118-specific transcripts is maintained until the end of the infectious cycle. The presence of a low level of specific transcripts corresponding to three other members of the multigene family 110, namely, X′82, U124, and U104, has also been detected at late times (20 h) postinfection. Furthermore, a transcriptional kinetics comparable to that of V118 has been observed with the p32 gene, an unrelated ASFV early gene. These findings could be explained as the result of a long half-life of the transcripts analyzed. However, the marked decrease in the amount of early transcripts detected between 8 and 10 h postinfection indicates that the mRNAs studied are rapidly degraded. Although other possibilities are likely, the presence of a low level of mRNAs corresponding to early genes during the late phase of the infectious cycle could be interpreted as the result of a basal transcriptional activity of the early promoters after the onset of virus DNA replication.

Transcriptional mapping of the members of the multigene family 110 has revealed the presence of five independent

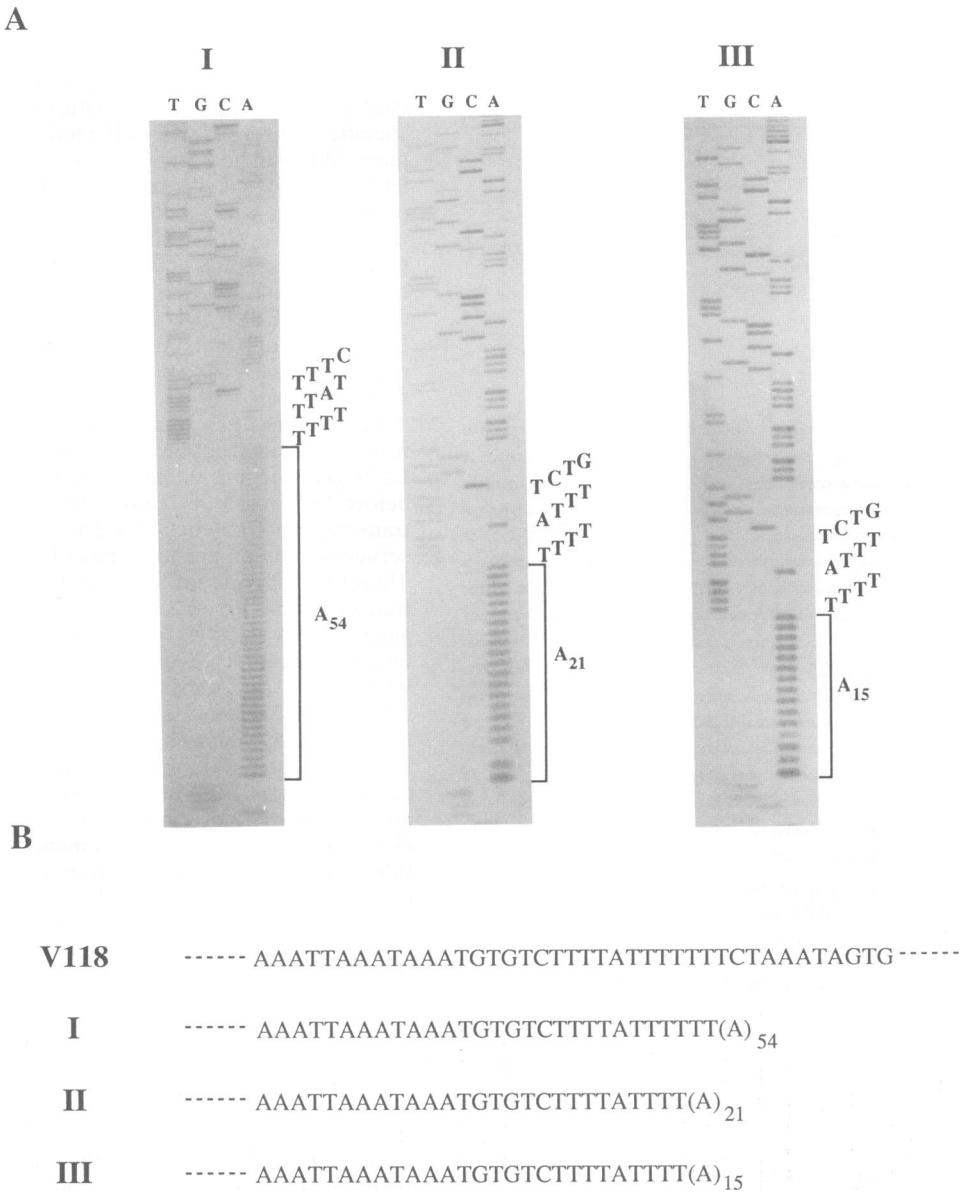

FIG. 8. 3′-end nucleotide sequences of V118 cDNAs. (A) Autoradiograms I, II, and III show the nucleotide sequences corresponding to the 3′ ends of the inserts of three recombinant M13 clones containing cDNAs generated from V118 mRNA. The letters at the top of each autoradiogram (A, C, G, and T) indicate the dideoxynucleotides used for the sequencing reactions. The lengths of the poly(A) tails and the nucleotide sequences immediately upstream of the poly(A) tails are indicated. (B) Nucleotide sequences of the DNA region located 30 to 80 nucleotides downstream of the V118 gene and the regions corresponding to the 3′ ends of V118 cDNA clones I, II, and III.

transcriptional units, thus indicating the existence of an accurate transcriptional control for each member of this small cluster of tandemly arranged genes. These five tightly packed nonoverlapping transcriptional units give rise to transcripts of defined length which initiate a short distance (8 to 70 bp) upstream of the corresponding ORF and terminate at one or more sites located downstream of the termination codon of the ORF. In all detected transcripts, the first AUG codon from the 5′ end coincides with the predicted translational initiation site of the gene (2), and the sizes of the different transcripts derived from the S1 nuclease analysis are in good agreement with those previously obtained by Northern blot hybridization (2).

Information about the precise locations of ASFV promoter sequences is not available. However, the fact that expression of the β-galactosidase gene of *E. coli* inserted within the genome of ASFV is accurately controlled by a short DNA sequence that corresponds to the upstream region of the ASFV p72 gene (17) indicates that it is very likely that ASFV promoters are located a short distance from the corresponding ORFs. A nucleotide sequence comparison of the DNA regions located immediately upstream of the genes studied did not reveal the presence of any conserved motifs that could provide clues about relevant sequences for promoter activity. It is important to point out that the regions located upstream of the V118, X′82, and

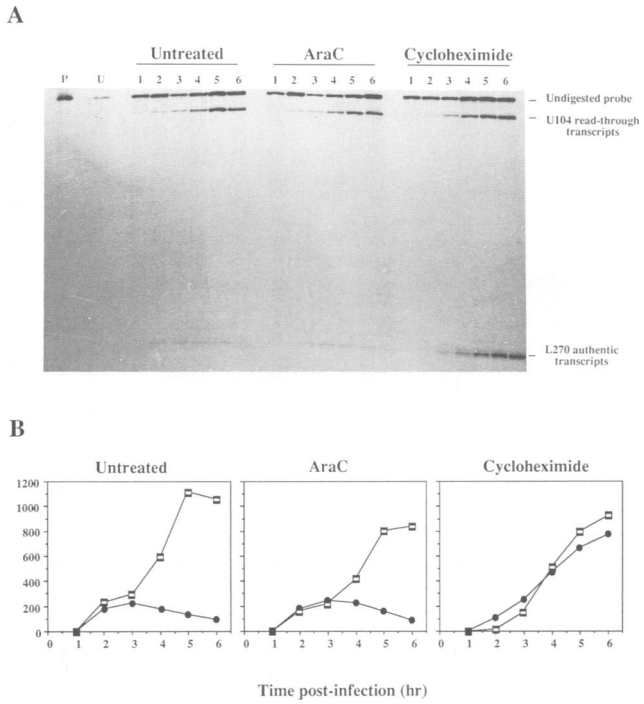

FIG. 9. Transcriptional kinetics of the L270 gene. (A) A ^{32}P-end-labeled probe (Fig. 6) was hybridized with 7.5 μg of total RNA extracted from untreated, AraC-treated, or cycloheximide-treated ASFV-infected Vero cells. The RNA-DNA hybrids were digested with S1 nuclease and subjected to electrophoresis. The positions of the undigested probe and the protected fragments corresponding to either readthrough transcripts from the U104 gene or L270 authentic transcripts are indicated. The numbers indicate the times postinfection (hours) at which the different RNA samples were extracted. Lanes P and U correspond to the undigested probe and the S1-digested RNA-DNA hybrids formed after incubation of RNA from uninfected Vero cells with the labeled probe. (B) Densitometric analysis of the autoradiogram shown in panel A. The intensities of the S1 nuclease-protected bands are plotted as the number of pixel units above the background detected for the corresponding band. The squares and circles correspond to U104 readthrough and L270 authentic transcripts, respectively.

U124 genes, respectively, are more than 95% identical. However, these regions are included within a series of repetitive sequences which span the 3.2-kb DNA fragment studied (2). Therefore, the high level of conservation observed among these sequences cannot be directly attributed to their potential regulatory function.

Recently, it has been shown that, after either stable insertion within the genome of vaccinia virus (VV), the prototype poxvirus, or transfection of ASFV DNA into VV-infected cells, faithful expression of some ASFV genes takes place (8). This indicates that VV *trans*-acting regulatory elements are capable of some degree of interaction with ASFV promoter sequences. Thus, it is conceivable that promoter sequences from ASFV share some of the features of the poxvirus promoters. A large number of VV early promoters have been characterized; they are short (30 to 40-bp), A-T-rich sequences located immediately upstream of the transcribed region of the corresponding gene (reviewed in reference 13). Interestingly, the average A-T content found within the 30-bp region immediately upstream of the transcriptional initiation sites of the members of the multigene family 110 (76%) is significantly higher than that found within the whole 3.2-kb DNA fragment in which these five genes are contained (63%). We hope that the use of systems to generate ASFV recombinants (17) will allow us to conduct the experiments necessary to define precisely the structure of ASFV promoter sequences.

S1 nuclease mapping of the 3′ ends of the five genes studied and nucleotide sequence analysis of three cDNA clones that correspond to the V118 gene revealed that the mRNAs terminate within one or more small DNA regions (5 to 11 bp) located a short distance from the termination codon of the corresponding ORF. The 3′ ends map within a strictly conserved sequence motif, formed by a run of seven or more consecutive thymidylate residues (7T), found within the intergenic regions. This suggests that the 7T motif might act as a signal for the 3′-end formation of these transcripts. Although the available information does not allow determination of the mechanism(s) involved in the 3′-end formation of ASFV mRNAs, the lack of the AAUAAA signal associated with the 3′-end processing of most eukaryotic mRNAs (16) in all but the transcripts from the V118 gene and the strong resemblance of the 7T motif to the signals for intrinsic termination found in both prokaryotic and eukaryotic systems, which in most cases are formed by T-rich regions in the nontranscribed DNA strand (reviewed in reference 9), suggest that mature ASFV early mRNAs might be generated by transcriptional termination followed by poly(A) addition. The detection of more than one 3′ end for transcripts from the U124 and L270 genes and the presence of V118 and U104 readthrough transcripts suggest that recognition of the first available 7T signal is not absolute; thus, transcripts with identical initiation sites can have different 3′ ends that map to alternative 7T motifs. The 7T sequence has a striking similarity to the 5TNT sequence which acts as a termination signal of early genes of poxviruses (19, 30). Indeed, the 7T motif would be functional if inserted within the context of a poxvirus genome. The large number of biochemical and genetic similarities found between poxviruses and ASFV (reviewed in reference 26) makes it tempting to speculate that the two virus groups have similar transcriptional mechanisms, including the sequence of the signal(s) involved in mRNA 3′-end formation. Transcriptional termination of early mRNAs of poxvirus has been thoroughly studied; it requires the presence of a transcriptional termination factor (VTF) (24), does not involve posttranscriptional cleavage events to generate mature mRNAs, and takes place 20 to 50 nucleotides downstream of the UUUUUNU sequence within the nascent mRNA molecule (31). The 3′ ends of the five ASFV genes analyzed fall within the 7T sequence, thus indicating at least one significant difference between the mechanisms of 3′-end formation used by the two virus groups. At first it seemed likely that the presence of a T residue in position 6 of the sequence motifs associated with the 3′ ends of the transcripts of the five ASFV genes analyzed in this study might not have statistical significance and that other ASFV genes might use the less stringent 5TNT motif as a signal for 3′-end formation of their corresponding mRNAs. Our results show that the only 5TVT motif (V stands for either A, C, or G) within the DNA region studied which does not overlap with a 7T motif does not correspond to any of the detected 3′ ends. However, the lack of recognition of the 5TVT sequence could be attributed to the sequestering, in a manner similar to that recently described for some VV early termination signals, of this motif within the mRNA secondary structure (12). Therefore, to assess further the likelihood of the 5TVT motif as an ASFV

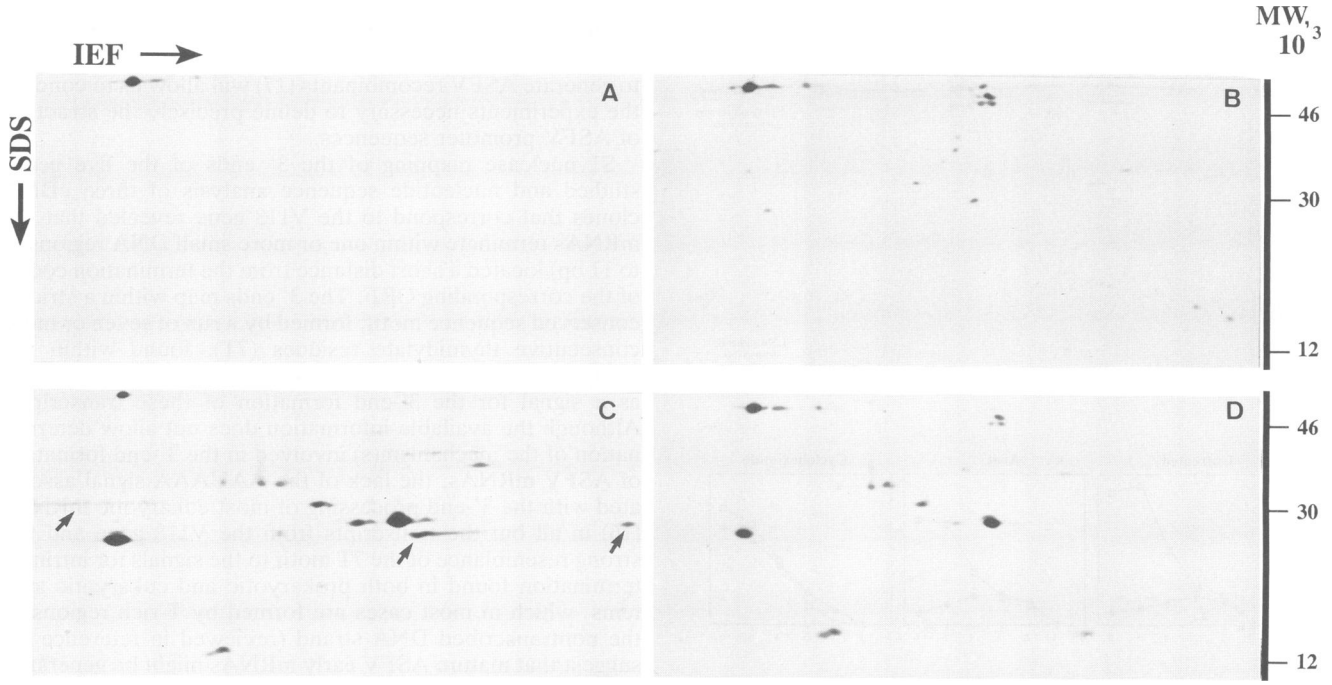

FIG. 10. Detection of virus-induced polypeptides encoded by genes whose transcription is silenced before the onset of virus DNA replication. The autoradiograms show the results of 2D gel electrophoresis of the [^{35}S]methionine-labeled polypeptides produced by in vitro translation in rabbit reticulocyte lysates programmed with H_2O (A), RNA from mock-infected Vero cells (B), or RNA from ASFV-infected Vero cells treated with either cycloheximide (C) or AraC (D). The directions of migration and the positions and sizes of molecular weight markers are indicated. The arrows (C) indicate the positions of radioactive spots which were detectable only after translation of RNA from cycloheximide-treated ASFV-infected cells. IEF, isoelectric focusing; SDS, sodium dodecyl sulfate.

termination signal, the frequency of the 7T and 5TVT motifs in either coding or noncoding regions of the ASFV DNA was analyzed (Table 1). The frequency of the 7T motif within intergenic regions is more than 40-fold higher than the frequency within intragenic sequences. However, a much smaller difference, only twofold, was found when a similar analysis was carried out for the 5TVT motif. This argues in favor of specific use of the 7T motif as a signal for transcriptional termination in ASFV. In addition, results recently obtained in our laboratory indicate that the 3′ ends of several late ASFV genes also map within 7T motifs (16a). Although transcriptional characterization of more ASFV genes is required to establish the functional role of the 7T motif unequivocally, the available data strongly suggest that the 7T sequence acts as a signal for 3′-end formation of ASFV mRNAs.

TABLE 1. Frequency of occurrence of 7T and 5TVT motifs within ASFV DNA

Sequence motif	Frequency of occurrence[a]		Ratio[b]
	Intergenic regions[c]	Intragenic regions[d]	
7T	6.082	0.148	41.09
5TVT	2.379	1.038	2.29

[a] The frequency of occurrence of either 7T or 5TVT (V stands for A, C, or G residues) motifs was determined by using an ASFV DNA data bank comprising all of the published sequences for which transcriptional information has been reported. The data bank included the region containing the *Eco*RI I fragment (17) and the 360 and 110 multigene families (2, 8). Frequency is expressed as the number of copies of the motif per kilobase of DNA.

[b] The ratio was determined by dividing the frequency of the motif within intergenic regions by the frequency within intragenic regions.

[c] The frequencies were calculated for both DNA strands within the regions corresponding to the spacing between the different ORFs and for the transcribed strand of the predicted ORFs. A total of 13,438 bp was analyzed.

[d] The frequencies were calculated for the nontranscribed strand of the predicted ORFs. A total of 11,345 bp was analyzed.

The results of transcriptional mapping of the L270 gene were surprising. While transcripts that correspond to the other four members of the 110 multigene family were detectable in all three types of RNA obtained from infected cells, authentic L270 transcripts were found only in immediate-early RNA. These results suggested that transcription of the L270 gene could be either induced by cycloheximide treatment or silenced very early during the infection as a result of de novo protein synthesis. The S1 nuclease analysis performed by using RNAs obtained at regular intervals during the first 6 h of infection demonstrates that transcription of the L270 gene is not an artifact caused by cycloheximide treatment. In both untreated and AraC-treated ASFV-infected cells, synthesis of authentic L270 transcripts started immediately after the beginning of infection and then, after 3 h, appeared to be slowly silenced. The silencing of L270 transcription was completely prevented by cycloheximide treatment. The results of 2D gel analysis of the polypeptide products obtained after in vitro translation of different types of RNA (uninfected, immediate-early, and early) showed that at least three virus-induced polypeptides are encoded by genes that can be classified as part of a subset of the early gene class whose transcription is abrogated before the onset of DNA replication. Transcription of this small subset might be controlled by the presence of a virus-encoded *trans-*

acting factor(s) synthesized at the beginning of infection. Alternatively, transcription of these genes may require the specific environment provided by the subvirion structure in which the virus DNA is enclosed during the initial steps of infection. Thus, silencing of these genes would be coincidental with disruption of the virus cores. Interestingly, a group of VV early genes showing characteristics similar to those of the subset we have described in ASFV was preliminarily characterized (5) but has since received very little attention.

Research on ASFV has been focused on the molecular biology of the virus. The work reported here represents an initial step of a systematic analysis that will, we hope, lead to a better understanding of the mechanisms that control the expression of ASFV genetic information.

ACKNOWLEDGMENTS

We thank Antonio Varas for skillful technical assistance and Katherine Law, Rafael Yáñez, and Maria L. Salas for critical reading of the manuscript.

This work was supported by grants from the Comisión Interministerial de Ciencia y Tecnología, the Junta de Extremadura, and the European Economic Community and by an institutional grant from the Fundación Ramón Areces. J.R. was a fellow of the Fondo de Investigaciones Sanitarias. F.A., G.A., and R.P. were fellows of the Ministerio de Educación y Ciencia.

REFERENCES

1. **Almeida, J. D., A. P. Waterson, and W. Plowright.** 1967. The morphological characteristics of African swine fever virus and its resemblance to Tipula iridescent virus. Arch. Gesamte Virusforsch. **20:**392–396.
2. **Almendral, J. M., F. Almazán, R. Blasco, and E. Viñuela.** 1990. Multigene families in African swine fever virus: family 110. J. Virol. **64:**2064–2072.
3. **Berk, A. J., and P. A. Sharp.** 1977. Sizing and mapping of early adenovirus mRNAs by gel electrophoresis of S1 endonuclease-digested hybrids. Cell **12:**721–732.
4. **Bravo, R.** 1984. Two-dimensional gel electrophoresis: a guide for the beginner, p. 3–36. *In* J. E. Celis and R. Bravo (ed.), Two dimensional gel electrophoresis of proteins: methods and applications. Academic Press, Inc., New York.
5. **Cooper, J. A., and B. Moss.** 1979. *In vitro* translation of immediate early, early, and late classes of RNA from vaccinia virus-infected cells. Virology **96:**368–380.
6. **Enjuanes, L., A. L. Carrascosa, M. A. Moreno, and E. Viñuela.** 1976. Titration of African swine fever (ASF) virus. J. Gen. Virol. **32:**471–477.
7. **González, A., V. Calvo, F. Almazán, J. M. Almendral, J. C. Ramírez, I. De La Vega, R. Blasco, and E. Viñuela.** 1990. Multigene families in African swine fever virus: family 360. J. Virol. **64:**2073–2081.
8. **Hammond, J. F., and L. K. Dixon.** 1991. Vaccinia virus-mediated expression of African swine fever virus genes. Virology **181:**778–782.
9. **Kerppola, T. K., and C. M. Kane.** 1991. RNA polymerase: regulation of transcript elongation and termination. FASEB J. **5:**2833–2842.
10. **Kuznar, J., M. L. Salas, and E. Viñuela.** 1980. DNA-dependent RNA polymerase in African swine fever virus. Virology **101:** 169–175.
11. **Laskey, R. A., and A. D. Mills.** 1975. Quantitative film detection of ^{3}H and ^{14}C in polyacrylamide gels by fluorography. Eur. J. Biochem. **56:**335–341.
12. **Luo, Y., and S. Shuman.** 1991. Antitermination of vaccinia virus early transcription: possible role of RNA secondary structure. Virology **185:**432–436.
13. **Moss, B.** 1990. Regulation of vaccinia virus transcription. Annu. Rev. Biochem. **59:**661–688.
14. **Moura Nunes, J. F., J. D. Vigario, and A. M. Terrinha.** 1975. Ultrastructural study of African swine fever virus replication in cultures of swine bone marrow cells. Arch. Virol. **49:**59–66.
15. **O'Farrel, P. H.** 1975. High resolution two-dimensional electrophoresis of proteins. J. Biol. Chem. **250:**4007–4021.
16. **Proudfoot, N. J.** 1989. How RNA polymerase II terminates transcription in higher eukaryotes. Trends Biochem. Sci. **14:** 105–110.

16a. **Rodriguez, J. F.** Unpublished data.

17. **Rodríguez, J. M., F. Almazán, E. Viñuela, and J. F. Rodriguez.** 1992. Genetic manipulation of African swine fever virus: construction of recombinants expressing the β-galactosidase gene. Virology **188:**67–76.
18. **Rodríguez, J. M., M. L. Salas, and E. Viñuela.** 1992. Genes homologous to ubiquitin-conjugating and eukaryotic transcription factor SII in African swine fever virus. Virology **186:**40–52.
19. **Rohrmann, G., and B. Moss.** 1985. Transcription of vaccinia virus early genes by a template-dependent soluble extract of purified virions. J. Virol. **56:**349–355.
20. **Salas, M. L., J. Kuznar, and E. Viñuela.** 1981. Polyadenylation, methylation and capping of the RNA synthesized *in vitro* by African swine fever virus. Virology **113:**484–491.
21. **Salas, M. L., J. Rey-Campos, J. M. Almendral, A. Talavera, and E. Viñuela.** 1986. Transcription and translation maps of African swine fever virus. Virology **152:**228–240.
22. **Sambrook, J., E. F. Fritsch, and T. Maniatis.** 1989. Molecular cloning: a laboratory manual, 2nd ed. Cold Spring Harbor Laboratory, Cold Spring Harbor, N.Y.
23. **Santarén, J., and E. Viñuela.** 1986. African swine fever virus-induced polypeptides in Vero cells. Virus Res. **5:**391–405.
24. **Shuman, S., S. S. Broyles, and B. Moss.** 1987. Purification and characterization of a transcription termination factor from vaccinia virus virions. J. Biol. Chem. **262:**12372–12380.
25. **Viñuela, E.** 1985. African swine fever virus. Curr. Top. Microbiol. Immunol. **116:**151–170.
26. **Viñuela, E.** 1987. Molecular biology of African swine fever virus, p. 31–49. *In* Y. Becker (ed.), African swine fever. Martinus Nijhoff Publishing, Boston.
27. **Wardley, R. C., S. G. Norley, C. V. Martinus, and M. J. P. Lawman.** 1987. The host response to African swine fever virus. Prog. Med. Virol. **34:**180–192.
28. **Wilkinson, P. J.** 1989. African swine fever virus, p. 17–37. *In* M. B. Pensaert (ed.), Virus infections of porcines. Elsevier Science Publishers B.V., Amsterdam.
29. **Yanisch-Perron, C., J. Vieira, and J. Messing.** 1985. Improved M13 phage cloning vectors and host strains: nucleotide sequences of the M13mp18 and pUC19 vectors. Gene **33:**103–119.
30. **Yuen, L., and B. Moss.** 1986. Multiple 3′ ends of mRNA encoding vaccinia virus growth factor occurs within a series of repeated sequences downstream of T clusters. J. Virol. **60:**320–323.
31. **Yuen, L., and B. Moss.** 1987. Oligonucleotide sequence signaling transcriptional termination of vaccinia virus early genes. Proc. Natl. Acad. Sci. USA **84:**6417–6421.